SACLANTCEN Report SR-41

(2)

43

SACLANTCEN Report
SR-41

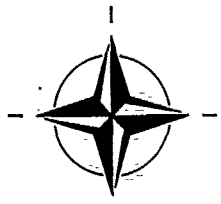

SACLANT ASW
RESEARCH CENTRE
REPORT

AD A094995

SPATIAL CORRELATION OF SURFACE-GENERATED NOISE IN A STRATIFIED OCEAN

by

WILLIAM A. KUPERMAN and FRANK INGENITO

1 OCTOBER 1980

DTIC
ELECTE
FEB 1 3 1981
S
A

NORTH
ATLANTIC
TREATY
ORGANIZATION

LA SPEZIA, ITALY

This document is unclassified. The information it contains is published subject to the conditions of the legend printed on the inside cover. Short quotations from it may be made in other publications if credit is given to the author(s). Except for working copies for research purposes or for use in official NATO publications, reproduction requires the authorization of the Director of SACLANTCEN.

DTIC FILE COPY

81 2 13 012

This document is released to a NATO Government at the direction of the SACLANTCEN subject to the following conditions:

1. The recipient NATO Government agrees to use its best endeavours to ensure that the information herein disclosed, whether or not it bears a security classification, is not dealt with in any manner (a) contrary to the intent of the provisions of the Charter of the Centre, or (b) prejudicial to the rights of the owner thereof to obtain patent, copyright, or other like statutory protection therefor.

2. If the technical information was originally released to the Centre by a NATO Government subject to restrictions clearly marked on this document the recipient NATO Government agrees to use its best endeavours to abide by the terms of the restrictions so imposed by the releasing Government.

(14) SACLANTCEN REPORT-SR-41

NORTH ATLANTIC TREATY ORGANIZATION

SACLANT ASW Research Centre
Viale San Bartolomeo 400, I-19026 San Bartolomeo (SP), Italy.

tel: national 0187 560940
international + 39 187 560940

telex: 271148 SACENT I

(11) 8 May 79

(12) 14

(6) SPATIAL CORRELATION OF SURFACE-GENERATED NOISE IN A STRATIFIED OCEAN

by

(10) William A. Kuperman and Frank Ingenito

(Reprinted from J.Acoustical Society America 67, 1980: 1988-1996)

1 October 1980

This report has been prepared as part of Project 19.

APPROVED FOR DISTRIBUTION

B.W. LYTHALL
Director

312950

PREFACE

The research reported in the paper reprinted within was started by the two authors at the U.S. Naval Research Laboratory, Washington, D.C. Soon after, one of the authors (W.A. Kuperman) transferred to SACLANTCEN where he performed most of his work. In addition, a complete computer model for performing the calculations has been developed at SACLANTCEN.

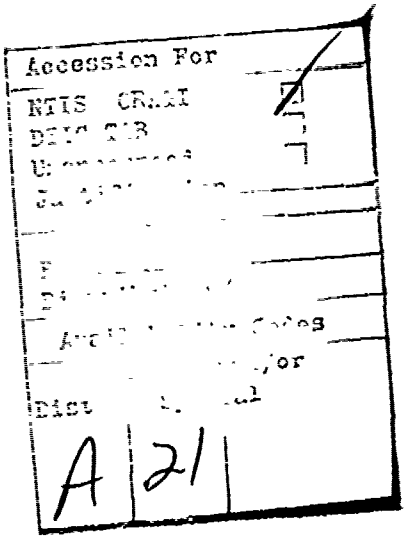

Spatial correlation of surface-generated noise in a stratified ocean

W. A. Kuperman

SACLANT ASW Research Centre, La Spezia, Italy
and Naval Research Laboratory, Washington, D.C. 20375

F. Ingenito

Naval Research Laboratory, Washington, D.C. 20375
(Received 8 May 1979; accepted for publication 3 March 1980)

A model is developed for the calculation of the spatial properties of the noise field produced in a stratified ocean by the action of wind at the surface. The random noise sources are represented by correlated monopoles distributed over an infinite plane located an arbitrary depth below the surface. Wave-theoretical methods are applied to derive expressions for the intensity and spatial correlation of the noise field. A normal-mode representation of the noise field is used to reduce these expressions to forms which allow physical interpretation and are suitable for numerical computation. Examples are given of intensity profiles and spatial correlation in the vertical for three generic sound-speed profiles. The results show that the sound-speed profile and the presence of the bottom can be important in determining the spatial properties of the noise field. An example is given of a calculation of the horizontal spatial correlation using the fast field program (FFP).

PACS numbers: 43.30.Nb, 43.30.Cq

INTRODUCTION

Detection of acoustic signals in the ocean is always performed against a noise background. Arrays of sensors may provide some discrimination against noise, the degree of discrimination being expressed by the array gain. The array gain, defined as the ratio of the signal to noise of the array output to the signal to noise of the output of a single element, can be shown to depend on the spatial correlation of the noise field.[1] In addition, recently developed optimal array processing techniques[2,3] require knowledge of the spatial correlation of the noise field.

One of the major components of the ambient noise field in the ocean is produced by the action of the wind at the surface. Previous theoretical studies of the spatial structure of surface generated noise have been carried out with deep water applications in mind.[4,5] Thus, the ocean has been modeled as a homogeneous half-space which allows straight-line propagation without reflection, greatly simplifying the calculation. Such models are of doubtful validity in shallow water where the acoustic field interacts strongly with the bottom. Cox[6] has pointed out that the assumption that noise arrives only from above the horizontal is counter to experimental evidence. He shows how the spatial structure of the noise field is related to a plane-wave directivity function in terms of a sum of angular harmonics. The coefficients of the harmonics can in turn be related to deep water experimental results. We note however that in deep or shallow water the sound speed is not constant in depth, a fact which may have a profound effect on the noise field, as it does on the signal field. Since the ocean is horizontally stratified it is quite possible that the acoustic field cannot be expressed in terms of the same weighted set of plane waves (same directivity function) at each of the hydrophones of an array, particularly a large aperture vertical array.

In this paper, using wave theory, we develop a model of surface generated noise in which the ocean is stratified in depth. The acoustic properties of the ocean bottom are included, as are the statistical properties of the surface. In Sec. I we derive a general expression based on wave theory for the cross-spectral density of surface generated noise. In Sec. II we apply this formalism using a normal-mode representation of the Green's function for the problem. This allows us to gain some physical insight into how the noise is spatially distributed. Section III presents some numerical results for realistic ocean environments. In Appendix A we show that the results derived in Sec. I reduce to earlier results[4] when the appropriate limits are taken. Finally, Appendix B presents some purely analytic results for an idealized waveguide.

I. DERIVATION OF THE SPATIAL PROPERTIES OF SURFACE GENERATED NOISE

The model geometry is shown in Fig. 1. The figure illustrates a simple case, with a layer of water overlying a semi-infinite bottom, the density and sound speed of the water and the bottom given by $\rho_1, c_1(z)$ and $\rho_2, c_2(z)$, respectively. The theory to be presented below is also applicable to more complex environments. For example, attenuation in the water and the bottom can be included as can a layered bottom with finite rigidity. Figure 1 is merely meant to suggest that the environment must be stratified in depth, thus ensuring separability of the wave equation. In the development below, we drop the subscripts distinguishing the sound speeds in the water and bottom and denote the sound speed anywhere in the medium by $c(z)$.

Consider an infinite plane parallel to the surface and located below the surface at depth z'. Assume that at each point in the plane there is a monopole source of strength $s(\mathbf{r}', t)$, where $\mathbf{r}'$ is the radial vector in the

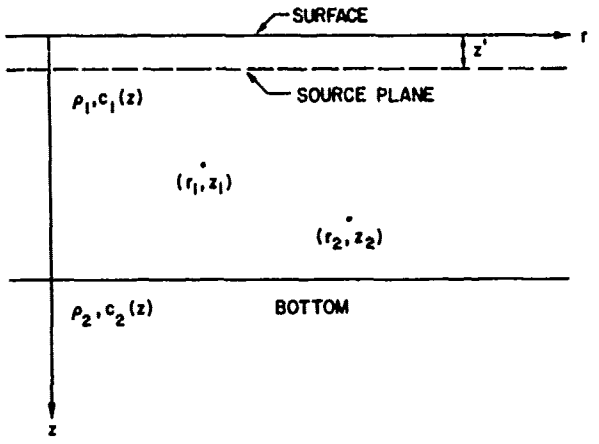

FIG. 1. The model geometry showing the source plane, at depth z' below the surface, and the two field points (r_1, z_1) and (r_2, z_2).

source plane and t is the time variable. Let the function $s(\mathbf{r}', t)$ be a random variable. These monopoles will couple into the water column as dipoles because of the pressure release surface; this effect is automatically incorporated in the wave-theoretic treatment used. We use monopole sources because they represent the basic fluctuating volume source[7] and more complicated sources can be considered to be a sum of these sources appropriately distributed in space. Therefore, the source function is $s(\mathbf{r}', t)\delta(z - z')$ so that the field (velocity potential) in the water column $\Phi(\mathbf{r}, z, t)$ satisfies the wave equation

$$\left(\nabla^2 - \frac{1}{c^2(z)}\frac{\partial^2}{\partial t^2}\right)\Phi = -s(\mathbf{r}', t)\delta(z - z'), \tag{1}$$

where $\delta(z)$ is the Dirac delta function.

We represent Φ and s by their Fourier transforms

$$\Phi(\mathbf{r}, z, t) = (2\pi)^{-1/2}\int_{-\infty}^{\infty} d\omega\, \varphi_\omega(\mathbf{r}, z)\exp(-i\omega t), \tag{2}$$

$$s(\mathbf{r}', t) = (2\pi)^{-1/2}\int_{-\infty}^{\infty} d\omega\, S_\omega(\mathbf{r}')\exp(-i\omega t), \tag{3}$$

where ω denotes angular frequency.

Inserting Eqs. (2) and (3) into Eq. (1), we obtain, after some manipulation,

$$(\nabla^2 + k^2)\varphi_\omega = -S_\omega(\mathbf{r}')\delta(z - z'); \quad k \equiv \omega/c(z). \tag{4}$$

Equation (4) has the solution

$$\varphi_\omega(\mathbf{r}, z) = \int d^2\mathbf{r}'\, S_\omega(\mathbf{r}')G(\mathbf{r}, \mathbf{r}'; z, z'), \tag{5}$$

where $G(\mathbf{r}, \mathbf{r}'; z, z')$, the Green's function of the problem, satisfies the Helmholtz equation

$$(\nabla^2 + k^2)G(\mathbf{r}, \mathbf{r}'; z, z') = -(1/r)\delta^2(\mathbf{r} - \mathbf{r}')\delta(z - z') \tag{6}$$

and the appropriate boundary conditions. Equation (5) simply states that the total velocity potential is obtained by summing over all source contributions. We note here that S_ω is the spectral strength of the noise sources and that the total field is given by integrating over all frequencies as stated in Eq. (2). In order to simplify notation, we shall usually drop the subscript ω.

The cross-spectral density is a measure of the spatial coherence of the noise field. To obtain the cross-spectral density we form the product of $\varphi(\mathbf{r}_1, z_1)$ and $\varphi^*(\mathbf{r}_2, z_2)$ and take the ensemble average (φ^* is the complex conjugate of φ). Thus,

$$\langle \varphi(\mathbf{r}_1, z_1)\varphi^*(\mathbf{r}_2, z_2)\rangle$$
$$= \int\int d^2\mathbf{r}'\, d^2\mathbf{r}''\langle S(\mathbf{r}')S^*(\mathbf{r}'')\rangle$$
$$\times G(\mathbf{r}_1, \mathbf{r}'; z_1, z')G^*(\mathbf{r}_2, \mathbf{r}''; z_2, z'), \tag{7}$$

where the angle brackets indicate an average taken over the random function S. It will be convenient to use a transverse Fourier representation of the Green's function[8] which we write as

$$G(\mathbf{r}, \mathbf{r}'; z, z')$$
$$= \frac{1}{2\pi}\int d^2\eta\, g(\eta; z, z')\exp[i\eta\cdot(\mathbf{r} - \mathbf{r}')], \tag{8}$$

where $g(\eta; z, z')$ satisfies the equation

$$\frac{d^2g}{dz^2} + [k^2(z) - \eta^2]g = -\frac{1}{2\pi}\delta(z - z'), \tag{9}$$

which follows from Eq. (6).

Using this Fourier representation, we can express the cross-spectral density function of the noise field as

$$\langle \varphi(\mathbf{r}_1, z_1)\varphi^*(\mathbf{r}_2, z_2)\rangle$$
$$= \int\int d^2\mathbf{r}'\, d^2\mathbf{r}''\langle S(\mathbf{r}')S(\mathbf{r}'')\rangle$$
$$\times \frac{1}{(2\pi)^2}\int\int d^2\eta\, d^2\eta' g(\eta; z_1, z')g^*(\eta'; z_2, z')$$
$$\times \exp[i\eta\cdot(\mathbf{r}_1 - \mathbf{r}')]\exp[-i\eta'\cdot(\mathbf{r}_2 - \mathbf{r}'')]. \tag{10}$$

Now let $\mathbf{R} = \mathbf{r}_1 - \mathbf{r}_2$ and $\boldsymbol{\rho} = \mathbf{r}' - \mathbf{r}''$, and assume that the spatial coherence of the noise sources, $\langle S(\mathbf{r}')S(\mathbf{r}'')\rangle$, depends only on $\boldsymbol{\rho}$. We denote $\langle S(\mathbf{r}')S(\mathbf{r}'')\rangle$ as $q^2N(\rho)$. Substituting for $\mathbf{r}_1$ and $\mathbf{r}'$ in Eq. (10), the integrations over $\mathbf{r}''$ and η' can be performed, resulting in

$$C_\omega(\mathbf{R}, z_1, z_2) \equiv \langle \varphi(\mathbf{r}_1, z_1)\varphi^*(\mathbf{r}_2, z_2)\rangle$$
$$= q^2\int\int d^2\rho\, d^2\eta N(\boldsymbol{\rho})g(\eta; z_1, z')$$
$$\times g^*(\eta; z_2, z')\exp[i\boldsymbol{\eta}\cdot(\mathbf{R} - \boldsymbol{\rho})], \tag{11}$$

where ω is used as a subscript to remind us that the cross-spectral density function depends on frequency. Since g and g^* depend on the magnitude of η, but not its direction [see Eq. (9)], we can perform the integration over the azimuthal angle associated with η, with the result that the cross-spectral density function takes the form

$$C_\omega(\mathbf{R}, z_1, z_2) = 2\pi q^2\int d\rho N(\rho)\int_0^\infty \eta\, d\eta\, g(\eta; z_1, z')$$
$$\times g^*(\eta; z_2, z')J_0(\eta|\mathbf{R} - \boldsymbol{\rho}|), \tag{12}$$

where J_0 is the Bessel function of zero order. Another form for C_ω, which is particularly simple, can be obtained by expressing $N'(\boldsymbol{\rho})$ by its Fourier transform

$P(\eta)$:

$$N(\rho)=\frac{1}{2\pi}\int d^2\eta\, P(\eta)e^{i\eta\cdot\rho}. \tag{13}$$

Then the integration over ρ in Eq. (11) can be performed, giving

$$C_\omega(\mathbf{R},z_1,z_2)=2\pi q^2\int d^2\eta\, P(\eta)g(\eta;z_1,z')\times g^*(\eta;z_2,z')e^{i\eta\cdot\mathbf{R}}. \tag{14}$$

Equation (12) can be put into a form which will be useful for later calculations by decomposing the Bessel function into a sum of Hankel functions

$$J_0(z)=\tfrac{1}{2}\left(H_0^{(1)}(z)+H_0^{(2)}(z)\right), \tag{15}$$

where the superscripts denote the Hankel function of first and second kind. Using the relation $-H_0^{(1)}(-z)=H_0^{(2)}(z)$ and noting that g and g^* are even in η we can extend the integration over η from $-\infty$ to ∞. Equation (12) becomes

$$C_\omega(\mathbf{R},z_1,z_2)=\pi q^2\int d\rho\, N(\rho)\int_{-\infty}^{\infty}\eta\, d\eta\, H_0^{(1)}(\eta|\mathbf{R}-\rho|)\times g(\eta;z_1,z')g^*(\eta;z_2,z'). \tag{16}$$

From the expressions for the cross-spectral density function of the noise field [Eqs. (12), (14), and (16)], we can immediately make some comments about its structure. In any horizontal plane, it is independent of absolute position and depends only on the horizontal vector R connecting the field points. In the vertical, the spatial coherence depends not only on separation distance but also on the absolute depth of the field points. Hence, in general, the noise is not spatially stationary in the vertical.

An important special case is that of uncorrelated noise sources. Equation (16) is an expression for the cross-spectral density function of the noise field as a function of the spatial coherence of the noise sources $N(\rho)$. For uncorrelated noise sources, it has been shown that[9]

$$N(\rho)=2\delta(\rho)/k^2\rho. \tag{17}$$

Using Eq. (17) in Eq. (16) we get

$$C_\omega(\mathbf{R},z_1,z_2)=4\pi^2q^2k^{-2}\int_{-\infty}^{\infty}\eta\, d\eta\, H_0^{(1)}(\eta R)\times g(\eta;z_1,z')g^*(\eta;z_2,z'). \tag{18}$$

When we set $R=0$ and $z_1=z_2=z$ in the expression for C_ω, we obtain a quantity proportional to the intensity of the noise field at a point. Equation (16) then reduces to

$$C_\omega(0,z,z)\equiv I_\omega(z)=\pi q^2\int d\rho\, N(\rho)\times\int_{-\infty}^{\infty}\eta\, d\eta\, H_0^{(1)}(\eta\rho)|g(\eta;z,z')|^2 \tag{19}$$

or alternatively, from Eq. (14),

$$I_\omega=2\pi q^2\int d^2\eta\, P(\eta)|g(\eta;z,z')|^2. \tag{20}$$

The expressions given by Eqs. (18), (19), and (20) will be useful later. We also mention for clarity in nomenclature that the correlation function of the noise field is given by

$$\langle\Phi(\mathbf{r}_1,z_1,t)\Phi^*(\mathbf{r}_2,z_2,t+\tau)\rangle=\int_{-\infty}^{\infty}C_\omega(\mathbf{R},z_1,z_2)\exp(-i\omega\tau)\,d\omega, \tag{21}$$

where τ is a time delay.

In this paper, we are mainly concerned with the distribution of noise in a stratified ocean, and in particular in situations where the acoustic properties of the ocean bottom have a profound effect on the acoustic field. Nevertheless, the model should also handle situations where the bottom is not important, for example, the deep ocean. In Appendix A we show that the above theoretical results reduce to earlier work[4] where the ocean was modeled as a semi-infinite isovelocity half-space.

II. NORMAL-MODE REPRESENTATION OF THE NOISE FIELD

In this section we apply the results of Sec. I to a stratified medium, that is a medium in which the sound velocity and density of the medium are functions of depth z only. The Green's function can be expressed in several equivalent ways; in this section we use a normal-mode representation in which the Green's function is expanded in terms of the normal modes of the system. If the medium is finite in depth with appropriate conditions given at the boundary, the normal modes will be discrete and the propagating modes will be finite in number. However, if the medium is infinite in depth, there will, in general, exist a finite number of discrete modes and an infinite set of continuous modes. The Green's function expansion will then consist of a discrete sum plus an integral over the continuous modes.

For simplicity, we restrict ourselves to that part of the noise field which can be represented by a discrete set of normal modes. From the above discussion we see that this will be a complete description for the pressure-release/rigid waveguide discussed in Appendix B, but not for more realistic ocean models. The latter usually consist of a layer of water and several sedimentary layers overlying a semi-infinite basement. However, by making the acoustic impedance of the basement very high, we can minimize the importance of the continuous modes.

The Green's function $g(\eta;z,z')$ can be written in terms of the normal modes as follows[8]:

$$g(\eta;z,z')=\frac{\rho_s(z')}{2\pi}\sum_n\frac{U_n(z')U_n(z)}{\eta^2-k_n^2}, \tag{22}$$

where $U_n(z)$ and k_n are the normalized mode amplitude function and the wavenumber of the nth mode and are solutions of the eigenvalue problem defined by the equation

$$\frac{d^2U_n(z)}{dz^2}+\left[k^2(z)-k_n^2\right]U_n(z)=0, \tag{23}$$

with the appropriate boundary conditions. In Eq. (22) $\rho_s(z')$ is the density of the medium at the depth z' and $k(z)=\omega/c(z)$ with $c(z)$ being the sound speed.

We assume that k_n is a complex number of the form

$$k_n = \kappa_n + i\alpha_n, \tag{24}$$

with $\kappa_n, \alpha_n \geq 0$; α_n, the imaginary part of k_n, is the modal attenuation coefficient. It is interesting to note that we must include attenuation in the system to obtain a finite cross-spectral density function. This is because sound trapped by the layered medium (represented by the discrete modes) suffers cylindrical spreading while the amount of energy radiated by the noise sources increases as the square of the range from the field points. Hence, the contribution to the intensity of distant sources increases with range and the total intensity diverges. Any amount of attenuation in the system will cause the intensity to decay exponentially with range and ensure convergence. It is important to note that the resulting cross-spectral density functions and intensities will depend on the attenuation chosen.

We now insert the Green's function of Eq. (22) into the expression for the cross-spectral density function [Eq. (16)] and evaluate the η integral. From Eq. (22) we see that the integral of Eq. (16) has simple poles at

$$\eta = \pm k_n, \pm k_m^*, \tag{25}$$

of which the poles at $+k_n$ and $-k_m^*$ are in the upper half-plane. Using standard methods of complex integration we close the contour in the upper half-plane with a semicircle of large radius and evaluate the residues of the integral. The result is

$$C_\omega(\mathbf{R}, z_1, z_2) = \frac{iq^2\rho_s^2(z')}{4} \int d\rho N(\rho) \times \sum_{n,m} U_n(z')U_n(z_1)U_m(z')U_m(z_2) \times f_{nm}[H_0^{(1)}(k_n|\mathbf{R}-\rho|) - H_0^{(1)}(-k_m^*|\mathbf{R}-\rho|)], \tag{26}$$

where

$$f_{nm} = 1/(k_n^2 - k_m^{*2}). \tag{27}$$

The quantity f_{nm} is a measure of the coherence between the normal modes which make up the noise field. For example, if f_{nm} vanishes for $n \neq m$, then the noise field reduces to an incoherent sum over the normal modes. Writing f_{nm} in terms of the complex k_n's and assuming that $\kappa_n \gg \alpha_n, \kappa_m \gg \alpha_m$, we get

$$f_{nm} = \begin{cases} 1/(\kappa_n^2 - \kappa_m^2) & \text{for } m \neq n, \\ 1/4i\alpha_n\kappa_n & \text{for } n = m. \end{cases} \tag{28}$$

We see that the $n = m$ terms in the sum of Eq. (26) become infinite in the absence of attenuation. This is due to the contributions of distant sources, as discussed above. The $n \neq m$ terms remain finite because they are products of different modes with rapidly oscillating phases which give negligible contribution from distant sources. Equation (28) also indicates that if the attenuation coefficients α_n are much smaller than the smallest separation between eigenvalues, then the noise field can be approximated by an incoherent sum of modes. This is often the case in shallow water. We can further simplify Eq. (26) by approximating k_n by its real part κ_n. Then Eq. (26) reduces to

$$C_\omega(\mathbf{R}, z_1, z_2) = \frac{q^2\rho_s(z')}{8} \int d\rho N(\rho) \times \sum_n \frac{U_n^2(z')U_n(z_1)U_n(z_2)}{\alpha_n\kappa_n} J_0(\kappa_n|\mathbf{R}-\rho|), \tag{29}$$

where we have neglected the $n \neq m$ terms. Finally, when the noise sources are completely uncorrelated, the cross-spectral density takes the simple form

$$C_\omega(\mathbf{R}, z_1, z_2) = \frac{\pi q^2\rho_s^2(z')}{2k^2} \sum_n \frac{[U_n(z')]^2U_n(z_1)U_n(z_2)}{\alpha_n\kappa_n} J_0(\kappa_n R). \tag{30}$$

From Eq. (29) and Eq. (30) it is obvious that the structure of the noise field is highly dependent on the attenuation; in shallow water the attenuation is usually dominated by the acoustic interaction with the bottom sediments.

In Appendix B we evaluate the cross-spectral density function for a case which can be done analytically: an isovelocity waveguide bounded above by a pressure-release surface and below by a rigid bottom. Though it is not very descriptive of a real ocean environment, the analytic calculations are helpful in understanding how surface noise is distributed in a waveguide.

III. NUMERICAL RESULTS AND EXAMPLES

In this section we present sample calculations which exhibit some of the properties of the spatial correlation and intensity of the noise field. Most of the calculations were made using the normal-mode representation of the noise field presented in Sec. II, but we emphasize that the model presented here is not bound to a specific representation; any wave-theoretical representation can be used. As an example, we will also give some results calculated by a modification of the fast field program[10] (FFP), where the function $g(\eta; z, z')$ is calculated directly and Eqs. (18) and (19) are used.

First we present three cases which illustrate the effect of sound-speed profile and frequency on the intensity and spatial coherence of the noise field. In all three cases the water depth is 50 m and the bottom consists of 20 m of sediment overlying a hard basement. The sound speed, density, and attenuation coefficient of the sedimentary layer are characteristic of sand–silt–clay.[11] The noise sources are assumed to be uncorrelated and located 0.5 m below the surface; they are equivalent to sources at the surface with $\cos\theta$ directionality.

The three sound-speed profiles: isovelocity, downward refracting, and upward refracting are shown in Fig. 2. The corresponding noise intensities are shown in Figs. 3, 4, and 5 as functions of depth for the frequencies 200, 400, and 800 Hz. The results for the isovelocity and downward-refracting cases are qualiatively similar. Both cases show decreasing noise intensity as a function of depth, with a faster rate of decrease for the higher frequencies. The intensity decrease is

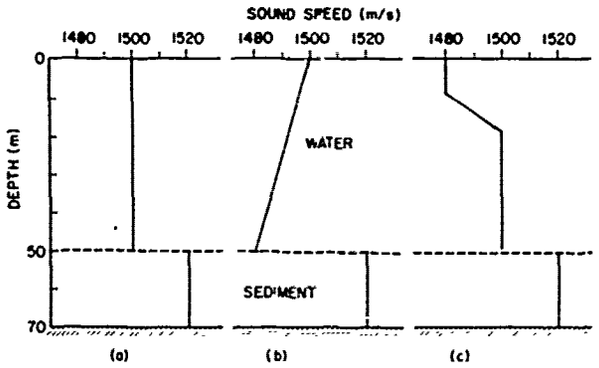

FIG. 2. Isovelocity, downward-refracting, and upward-refracting sound-speed profiles used in the calculations.

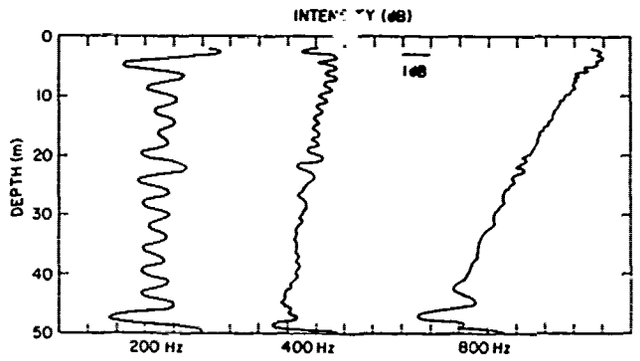

FIG. 4. Noise intensity as a function of depth for the downward-refracting profile shown in Fig. 2(b) and for the frequencies 200, 400, and 800 Hz.

caused by the frequency-dependent attenuation of the system. For the downward-refracting profile the attenuation, which is dominated by the bottom, is greater, resulting in a more rapid decrease. The peak in intensity which appears at all three frequencies in the upward-refracting case is caused by the low-order modes, which are the dominant contributors to the intensity. The low-order modes are trapped in the upper part of the water column and hardly interact with the bottom. Thus, their attenuations are very small and contributions from distant sources are important. The dominant low-order modes are strongest in the upper part of the water column, resulting in the observed peak.

For the noise intensity plots shown in Figs. 3, 4, and 5 no absolute levels are given. The model does not predict the levels of the noise sources, expressed by q^2 in Eq. (11), which we expect to be dependent on frequency. For the purposes of these calculations q^2 has been set equal to unity in all cases.

Figures 6, 7, and 8 show the spatial correlation function for the same cases as above. (For a single frequency and zero time delay the spatial correlation function is equal to the real part of the cross-spectral density.) For comparison the results for surface sources having $\cos\theta$ directionality in a semi-infinite homogeneous medium (Cron and Sherman[4] and Appendix A) are also shown. Again the upward-refracting case is the most interesting. In this case, as mentioned above, a few low-order modes dominate the noise field, resulting in high values of coherence throughout the water column. In the isovelocity and downward-refracting cases many modes contribute to the noise field and the coherence is much closer to the Cron and Sherman results.

Finally, we give a calculation of the spatial correlation in the horizontal direction. We have assumed an isovelocity water layer 100 m thick with a sound speed of 1500 m/s and a single semi-infinite bottom of unit density, sound speed of 1600 m/s, and an attenuation coefficient of 1 dB/λ. Figure 9 shows the horizontal spatial correlation at 100 Hz along with the Cron and Sherman result for comparison. For this environment the model spectrum consists of a discrete part and a continuous part, both of which contribute to the noise field. The correlation was calculated using a combination of the normal-model and FFP methods. Thus, Eq. (26) was used for the discrete normal-mode part and a modification of Eq. (18) was used for the continuous-mode part. In Fig. 10 we have plotted the discrete and the continuous contributions separately, both normalized, to illustrate the differences between the two contributions. The continuous part, while more coherent

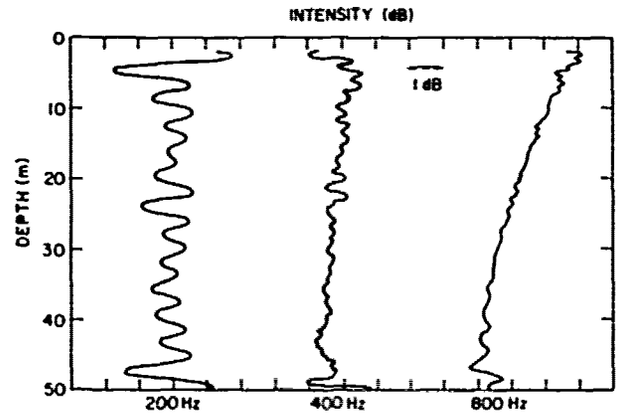

FIG. 3. Noise intensity as a function of depth for the isovelocity profile shown in Fig. 2(a) and for the frequencies 200, 400, and 800 Hz.

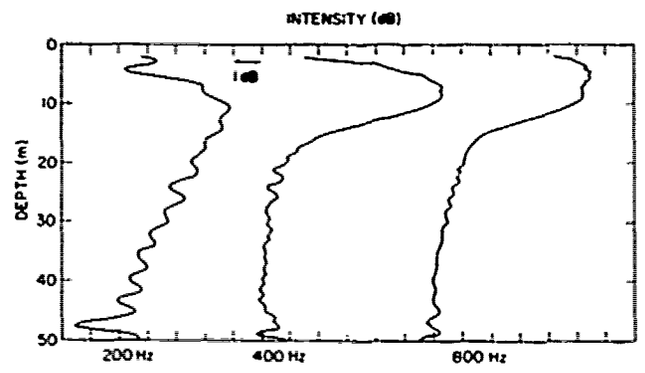

FIG. 5. Noise intensity as a function of depth for the upward-refracting profile shown in Fig. 2(c) and for the frequencies 200, 400, and 800 Hz.

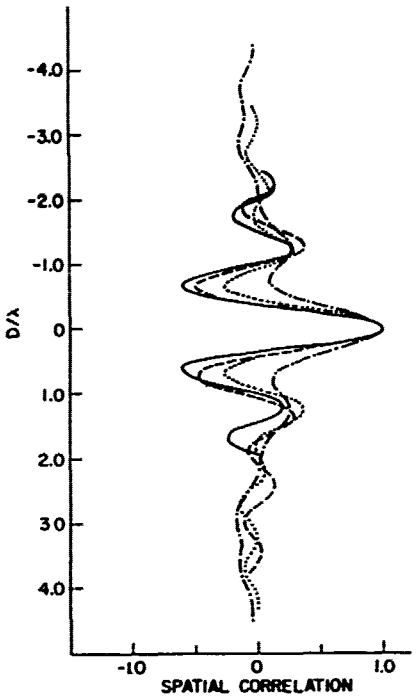

FIG. 6. Vertical spatial correlation functions for the isovelocity profile shown in Fig. 2(a) as a function of D/λ, where D is the receiver separation, λ the acoustic wavelength, and with one receiver fixed at 20-m depth. Three frequencies are shown: — 200 Hz; ••• 400 Hz; and –•–•– 800 Hz. Also shown is the result for a semi-infinite homogeneous medium calculated from Eq. (A22): ——.

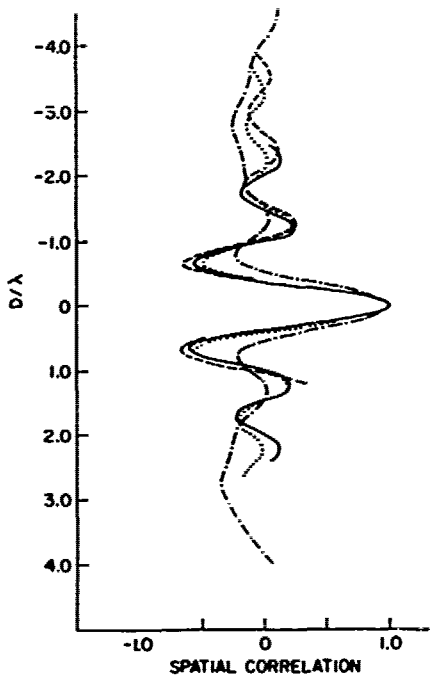

FIG. 7. Vertical spatial correlation functions for the downward-refracting profile shown in Fig. 2(b) as a function of D/λ, where D is the receiver separation, λ the acoustic wavelength, and with one receiver fixed at 40 m. Three frequencies are shown: — 200 Hz; ••• 400 Hz; and –•–•– 800 Hz. Also shown is the resul. for a semi-infinite homogeneous medium calculated from Eq. (A22): ——.

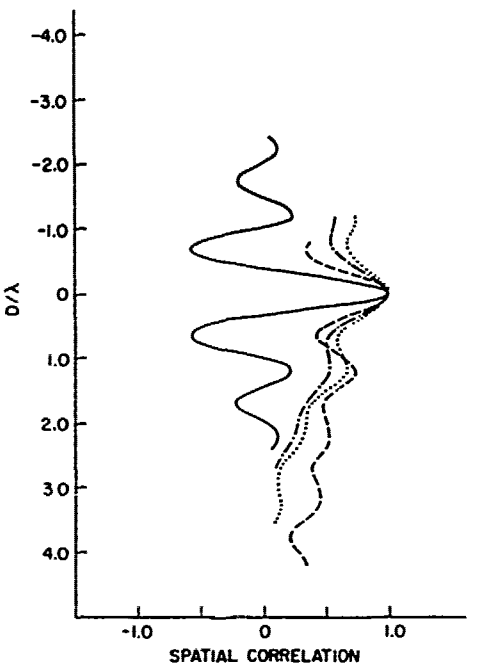

FIG. 8. Vertical spatial correlation functions for the upward-refracting profile shown in Fig. 2(c) as a function of D/λ, where D is the receiver separation, λ the acoustic wavelength, and with one receiver fixed at 10 m. Three frequencies are shown: — 200 Hz; ••• 400 Hz; and –•–•– 800 Hz. Also shown is the result for a semi-infinite homogeneous medium calculated from Eq. (A22): ——.

for small receiver separations (relative to a wavelength), quickly becomes less coherent than the discrete part, the latter maintaining some degree of coherence over several wavelengths.

The relative importance of the discrete and continuous parts of the normal-mode spectrum is dependent on the total loss of the system. For low loss the discrete

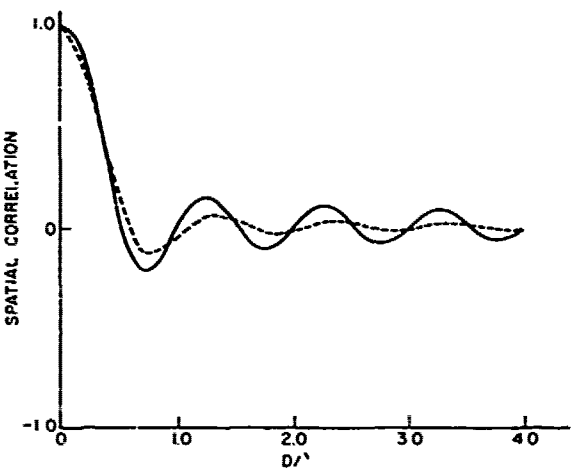

FIG. 9. Horizontal correlation function (solid line) for an isovelocity water layer overlying an isovelocity semi-infinite bottom as a function of D/λ, where D is the receiver separation and λ is the acoustic wavelength. The dashed line is the result for a semi-infinite, homogeneous medium [Eq. (A18) with $m = 1$].

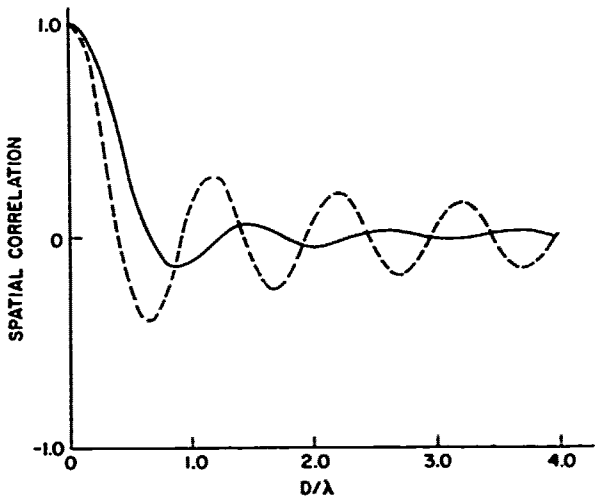

FIG. 10. The horizontal spatial correlation for the same case as Fig. 9 showing the discrete (——) and continuous (——) contributions, both normalized.

modes dominate, as they can be propagated very large distances from a very large area. In high-loss cases the continuous modes tend to dominate since they are important near the source while the long-range contributions of the discrete modes are severely attenuated.

IV. SUMMARY

We have presented a model of surface generated noise in the ocean in which the random noise sources are represented by correlated monopoles distributed over an infinite plane parallel to, and located on arbitrary depth below, the ocean surface. Expressions have been derived for the intensity and spatial coherence of the noise field in a stratified medium based on a wave-theoretical treatment. Examples have been given which demonstrate that environmental factors, such as the sound-speed profile and the presence of the bottom, can be important in determining the spatial properties of the noise field. We have also shown that for an isovelocity, semi-infinite fluid medium our results are identical to those of previous investigators.

ACKNOWLEDGMENT

This work was supported in part by NAVSEASYSCOM (Code 06H1-4).

APPENDIX A: SPATIAL COHERENCE IN A HOMOGENEOUS SEMI-INFINITE SPACE

In this appendix we show analytically that the theory developed in Sec. I reduces to earlier work[4] where the ocean was modeled as a semi-infinite space. For this problem, the Green's function is

$$G(\mathbf{r}_1,\mathbf{r}';z_1,z') = \frac{1}{4\pi}\frac{e^{ikR}}{R} - \frac{1}{4\pi}\frac{e^{ikR'}}{R'}, \tag{A1}$$

where

$$R = [\,|\mathbf{r}_1-\mathbf{r}'|^2+(z_1-z')^2\,]^{1/2}, \tag{A2}$$

and

$$R' = [\,|\mathbf{r}_1-\mathbf{r}'|^2+(z_1+z')^2\,]^{1/2},$$

and $k=\omega/c$, where ω is the angular frequency of the source and c is the speed of sound in the medium. The Green's function in Eq. (A1) is just that of a point source and its image, with the negative sign to satisfy the boundary condition at the surface,

$$G(\mathbf{r}_1,\mathbf{r}';0,z') = 0. \tag{A3}$$

To obtain $g(\eta;z_1,z')$ we note that[12]

$$\frac{1}{4\pi}\frac{e^{ikR}}{R} = \frac{i}{8\pi^2}\int_{-\infty}^{\infty}\int_{-\infty}^{\infty}\exp\{i[\boldsymbol{\eta}\cdot(\mathbf{r}_1-\mathbf{r}')+\eta_z|z_1-z'|]\}\frac{d^2\eta}{\eta_z}, \tag{A4}$$

where

$$\eta_z = (k^2-\eta^2)^{1/2} \quad \text{for } k^2>\eta^2,$$
$$= i(\eta^2-k^2)^{1/2} \quad \text{for } k^2<\eta^2.$$

Thus it follows from Eq. (8) that

$$g(\eta;z_1,z') = \frac{i}{4\pi}\left(\frac{\exp(i\eta_z|z_1-z'|)-\exp(i\eta_z|z_1+z'|)}{\eta_z}\right). \tag{A5}$$

Similarly we have that

$$g^*(\eta;z_2,z') = \frac{-i}{4\pi}\left(\frac{\exp(-i\eta_z^*|z_2-z'|)-\exp(-i\eta_z^*|z_2+z'|)}{\eta_z^*}\right). \tag{A6}$$

We are concerned with the case $z_1,z_2>z'$. Then, from Eqs. (A5) and (A6),

$$g(\eta;z_1,z')g^*(\eta;z_2,z') = \frac{1}{4\pi^2}\frac{\exp[i(\eta_z z_1-\eta_z^* z_2)]\sin(\eta_z z')\sin(\eta_z^* z')}{|\eta_z|^2}. \tag{A7}$$

Inserting Eq. (A7) in Eq. (12) we obtain the expression for the cross-spectral density function

$$C_{ww}(\mathbf{R},z_1,z_2) = \frac{1}{2\pi^2}q^2\int_0^{\infty}d^2\boldsymbol{\rho}N(\boldsymbol{\rho})\left(\int_0^{\infty}\eta\,d\eta J_0(\eta|\mathbf{R}-\boldsymbol{\rho}|)\times\frac{\exp[i(\eta_z z_1-\eta_z^* z_2)]\sin(\eta_z z')\sin(\eta_z^* z')}{|\eta_z|^2}\right). \tag{A8}$$

If k is real, the integral inside the large parentheses can be written

$$\int_0^{k}J_0(\eta|\mathbf{R}-\boldsymbol{\rho}|)\exp[i(z_1-z_2)(k^2-\eta^2)^{1/2}]\times\frac{\sin^2[z'(k^2-\eta^2)^{1/2}]}{k^2-\eta^2}\eta\,d\eta + \int_k^{\infty}J_0(\eta|\mathbf{R}-\boldsymbol{\rho}|)\exp[-(z_1+z_2)(\eta^2-k^2)^{1/2}]\times\frac{\sinh^2[z'(\eta^2-k^2)^{1/2}]}{\eta^2-k^2}\eta\,d\eta. \tag{A9}$$

We now must make some assumption about $N(\rho)$. Cron and Sherman[4] have calculated the correlation func-

tion for a homogeneous half-space with noise sources having $\cos^m\theta$ directionality distributed uniformly over the surface. Liggett and Jacobson[5] have shown that $\cos^m\theta$ directionality is equivalent to assuming omnidirectional sources with a correlation function given by

$$N(\rho) = 2^m m!(k\rho)^{-m} J_m(k\rho), \tag{A10}$$

for $m \geq 1$. Inserting Eq. (A10) in Eq. (A8), the angular part of the ρ integration can be performed, resulting in the expression

$$C_\omega(R; z_1, z_2) = q^2 2^m m! k^{-m} \left(\int_0^k F_m(\eta) J_0(\eta R) \exp[iZ(k^2-\eta^2)^{1/2}] \frac{\sin^2[z'(k^2-\eta^2)^{1/2}]}{k^2-\eta^2} \eta \, d\eta \right.$$
$$\left. + \int_k^\infty F_m(\eta) J_0(\eta R) \exp[-(z_1+z_2)(\eta^2-k^2)^{1/2}] \frac{\sinh^2[z'(\eta^2-k^2)^{1/2}]}{\eta^2-k^2} \eta \, d\eta \right). \tag{A11}$$

where $Z = z_1 - z_2$. $F_m(\eta)$ is known, and is given by[13]

$$F_m(\eta) = \int_0^\infty J_m(k\rho) J_0(\eta\rho) \rho^{1-m} \, d\rho$$
$$= \begin{cases} 0 & \text{for } k < \eta, \\ [2^{-1}(k^2-\eta^2)]^{m-1} k^{-m} [\Gamma(m)]^{-1} & \text{for } k \geq \eta. \end{cases} \tag{A12}$$

Thus, using Eq. (A12), Eq. (A11) becomes

$$C_\omega(R; z_1, z_2) = q^2 2mk^{-2m} \int_0^k (k^2-\eta^2)^{m-1} J_0(\eta R) \times \exp[iZ(k^2-\eta^2)^{1/2}] \times \frac{\sin^2[z'(k^2-\eta^2)^{1/2}]}{k^2-\eta^2} \eta \, d\eta. \tag{A13}$$

To compare with Cron and Sherman's results, we let $z' \to 0$ and take the normalized function $\bar{C}_\omega(R; z_1, z_2)$. Thus (Re denotes the real part)

$$\bar{C}_\omega(R; z_1, z_2) \equiv \lim_{z' \to 0} \frac{\mathrm{Re}[C_\omega(R; z_1, z_2)]}{\{\mathrm{Re}[C_\omega(0; z_1, z_1)] \mathrm{Re}[C_\omega(0; z_2, z_2)]\}^{1/2}}. \tag{A14}$$

Then we must evaluate the integral

$$I_m(R, Z) = \int_0^k (k^2-\eta^2)^{m-1} J_0(\eta R) \cos[Z(k^2-\eta^2)^{1/2}] \eta \, d\eta. \tag{A15}$$

First consider the case when $z_1 = z_2$. Then we have

$$I_m(R, 0) = \int_0^k (k^2-\eta^2)^{m-1} J_0(\eta R) \eta \, d\eta. \tag{A16}$$

This is a standard integral and is given by[14]

$$I_m(R, 0) = 2^{m-1} k^m R^{-m} (m-1)! J_m(kR). \tag{A17}$$

Therefore,

$$\bar{C}_\omega(R; z_1, z_1) = 2^m m! J_m(kR)/(kR)^m, \tag{A18}$$

which is just the correlation function of the surface, Eq. (A10).

Next, let $R = 0$. Then Eq. (A15) reduces to

$$I_m(0, Z) = \int_0^k (k^2-\eta^2)^{m-1} \cos[Z(k^2-\eta^2)^{1/2}] \eta \, d\eta. \tag{A19}$$

which, after changing to the variable ζ, where $\zeta = (k^2-\eta^2)^{1/2}$, becomes

$$I_m(0, Z) = \int_0^k \zeta^{2m-1} \cos(Z\zeta) \, d\zeta. \tag{A20}$$

For $m = 1$, the integral is easily calculated. The result is

$$I_1(0, Z) = kZ^{-1} \sin(kZ) + Z^{-2}[\cos(kZ) - 1]. \tag{A21}$$

Thus, we have, for $m = 1$,

$$\bar{C}_\omega(0, Z) = 2(kZ)^{-1} \sin(kZ) + 2(kZ)^{-2}[\cos(kZ) - 1]. \tag{A22}$$

For $m > 1$ we note that

$$I_m(0, Z) = (-1)^{m-1} \frac{\partial^{2m-2}}{\partial Z^{2m-2}} I_1(0, Z); \tag{A23}$$

so for $m \geq 1$

$$\bar{C}_\omega(0, Z) = (-1)^{m-1} 2_m k^{-2m} \frac{\partial^{2m-2}}{\partial Z^{2m-2}} I_1(0, Z). \tag{A24}$$

The results expressed by Eqs. (A18), (A22), and (A24) are in agreement with those of Cron and Sherman.

A comment is in order about the significance of the second integral in the large parentheses of Eq. (A11). Because of the source correlation function chosen [see Eq. (A10)], the second integral vanishes. We could have taken the sources to be completely uncorrelated by using the $N(\rho)$ given by Eq. (17); then each source would be equivalent to an independent dipole. The first term of Eq. (A11) would then give Cron and Sherman's results, while the second term, which can easily be calculated, would be negligible except near the surface. The second term therefore is the contribution of the nearfield of the dipoles.

APPENDIX B: A SIMPLE NORMAL-MODE EXAMPLE

As an illustration of the normal-mode representation of the noise field we consider an isovelocity waveguide of depth H bounded above by a pressure-release surface and below by a rigid bottom. The boundary conditions for this problem are

$$U_n(0) = 0 \tag{B1a}$$

and

$$\left. \frac{dU_n(z)}{dz} \right|_{z=H} = 0, \tag{B1b}$$

where the functions $U_n(z)$ satisfy Eq. (23). The solution

of Eqs. (23) and (B1) is

$$U_n(z) = (2/H)^{1/2} \sin(\lambda_n z), \tag{B2}$$

with

$$k_n^2 = k^2 - \lambda_n^2, \tag{B3}$$

where

$$\lambda_n = \left(\frac{2n-1}{2}\ \frac{\pi}{H}\right), \quad n = 1, 2, 3, \ldots . \tag{B4}$$

We introduce attenuation into the system by letting the wavenumber $k = \omega/c$ be complex:

$$k = \kappa + i\epsilon \tag{B5}$$

with ϵ, the plane-wave attenuation coefficient, taken to be a small positive number. Equation (B3) indicates that the modal wavenumber k_n must also be complex. Thus, we let

$$k_n = \kappa_n + i\alpha_n. \tag{B6}$$

The modal attenuation coefficient α_n can be shown by a similar method to that of the Appendix of Ref. 15, to be given by

$$\alpha_n = \frac{\epsilon}{\kappa_n} \int_0^H \kappa(z) |U_n(z)|^2 \, dz, \tag{B7}$$

for the general case of a depth-dependent sound velocity profile $c(z) = \omega/\kappa$. In the case considered here, $c(z) = c$ a constant, so Eq. (B7) reduces to

$$\alpha_n = \epsilon\kappa/\kappa_n. \tag{B8}$$

Substituting (B2) and (B8) into Eq. (30) we obtain the simple result

$$C_\omega(\mathbf{R}, z_1, z_2) = 2\pi q^2 \rho_s^2(z')/\epsilon\kappa^3 H^2 \sum_n \sin^2(\lambda_n z') \sin(\lambda_n z_1) \times \sin(\lambda_n z_2) J_0(\kappa_n R). \tag{B9}$$

We note that the attenuation coefficient ϵ appears in Eq. (B9) just as a scaling factor and does not affect the form of the cross-spectral density function. This is a result of the simple example chosen. In general, the factor $(\alpha_n \kappa_n)^{-1}$, which weighs each term in the sum will not be a constant, but will depend on n.

[1] R. J. Urick, *Principles of Underwater Sound for Engineers* (McGraw-Hill, New York, 1967), Sec. 3.8.
[2] J. Capon, Proc. IEEE 57, 1408–1418 (1969).
[3] A. B. Baggeroer, J. Acoust. Soc. Am. Suppl. 1 62, S30 (A) (1977).
[4] B. F. Cron and C. H. Sherman, J. Acoust. Soc. Am. 34, 1732–1736 (1962).
[5] W. S. Liggett and M. J. Jacobsen, J. Acoust. Soc. Am. 38, 303–312 (1965).
[6] H. Cox, J. Acoust. Soc. Am. 54, 1289–1301 (1973).
[7] D. Ross, *Mechanics of Underwater Noise* (Pergamon, New York, 1976), p. 4.
[8] W. A. Kuperman and F. Ingenito, J. Acoust. Soc. Am. 61, 1178–1187 (1977).
[9] M. J. Beran and G. B. Parrent, Jr., *Theory of Partial Coherence* (Prentice-Hall, Englewood Cliffs, 1964), p. 58.
[10] H. W. Kutschale, "Rapid Computation by Wave Theory of Propagation Loss in the Arctic Ocean," Lamont-Doherty Geological Observatory of Columbia University, CU-8-73, Tech. Rpt. No. 8 (March 1973).
[11] E. L. Hamilton, J. Geophys. Res. 75, 4423–4446 (1970); Geophysics 37, 620–646 (1972).
[12] L. M. Brekhovskikh, *Waves in Layered Media* (Academic, New York, 1960), p. 239.
[13] F. Oberhettinger, *Tables of Bessel Transformations* (Springer-Verlag, New York, 1972), p. 80.
[14] Reference 13, p. 39.
[15] F. Ingenito, J. Acoust. Soc. Am. 53, 858–863 (1973).

INITIAL DISTRIBUTION

	Copies
MINISTRIES OF DEFENCE	
MOD Belgium	2
DND Canada	10
CHOD Denmark	8
MOD France	8
MOD Germany	15
MOD Greece	11
MOD Italy	10
MOD Netherlands	12
CHOD Norway	10
MOD Portugal	5
MOD Turkey	5
MOD U.K.	16
SECDEF U.S.	61
NATO AUTHORITIES	
Defence Planning Committee	3
NAMILCOM	2
SACLANT	10
SACLANTREPEUR	1
CINCWESTLANT/COMOCEANLANT	1
COMIBERLANT	1
CINCEASTLANT	1
COMSUBACLANT	1
COMMAIREASTLANT	1
SACEUR	2
CINCNORTH	1
CINCSOUTH	1
COMNAVSOUTH	1
COMSTRIKFORSOUTH	1
COMEDCENT	1
COMMARAIRMED	1
CINCHAN	1

	Copies
SCNR FOR SACLANTCEN	
SCNR Belgium	1
SCNR Canada	1
SCNR Denmark	1
SCNR Germany	1
SCNR Greece	1
SCNR Italy	1
SCNR Netherlands	1
SCNR Norway	1
SCNR Portugal	1
SCNR Turkey	1
SCNR U.K.	1
SCNR U.S.	2
SECGEN Rep. SCNR	1
NAMILCOM Rep. SCNR	1
NATIONAL LIAISON OFFICERS	
NLO Canada	1
NLO Denmark	1
NLO Germany	1
NLO Italy	1
NLO U.K.	1
NLO U.S.	1
NLR TO SACLANT	
NLR Belgium	1
NLR Canada	1
NLR Denmark	1
NLR Germany	1
NLR Greece	1
NLR Italy	1
NLR Netherlands	1
NLR Norway	1
NLR Portugal	1
NLR Turkey	1
NLR UK	1
NLR US	1
Total initial distribution	236
SACLANTCEN Library	10
Stock	34
Total number of copies	280